THE JOURNAL OF BIOLOGICAL CHEMISTRY
Vol. 276, No. 26, Issue of June 29, pp. 23349–23356, 2001

Printed in U.S.A.

Calmodulin Activates Intersubunit Electron Transfer in the Neuronal Nitric-oxide Synthase Dimer*

Received for publication, January 24, 2001, and in revised form, April 6, 2001
Published, JBC Papers in Press, April 26, 2001, DOI 10.1074/jbc.M100687200

Koustubh Panda, Sanjay Ghosh, and Dennis J. Stuehr‡

From the Department of Immunology, Lerner Research Institute, Cleveland Clinic, Cleveland, Ohio 44195

Neuronal nitric oxide synthase (nNOS) is composed of an oxygenase domain that binds heme, (6*R*)-tetrahydrobiopterin, and Arg, coupled to a reductase domain that binds FAD, FMN, and NADPH. Activity requires dimeric interaction between two oxygenase domains and calmodulin binding between the reductase and oxygenase domains, which triggers electron transfer between flavin and heme groups. We constructed four different nNOS heterodimers to determine the path of calmodulin-induced electron transfer in a nNOS dimer. A predominantly monomeric mutant of rat nNOS (G671A) and its Arg binding mutant (G671A/E592A) were used as full-length subunits, along with oxygenase domain partners that either did or did not contain the E592A mutation. The E592A mutation prevented Arg binding to the oxygenase domain in which it was present. It also prevented NO synthesis when it was located in the oxygenase domain adjacent to the full-length subunit. However, it had no effect when present in the full-length subunit (*i.e.* the subunit containing the reductase domain). The active heterodimer (G671A/E592A full-length subunit plus wild type oxygenase domain subunit) showed remarkable similarity with wild type homodimeric nNOS in its catalytic responses to five different forms and chimeras of calmodulin. This reveals an active involvement of calmodulin in supporting transelectron transfer between flavin and heme groups on adjacent subunits in nNOS. In summary, we propose that calmodulin functions to properly align adjacent reductase and the oxygenase domains in a nNOS dimer for electron transfer between them, leading to NO synthesis by the heme.

Nitric oxide (NO)[1] acts as a vital signal and cytotoxic molecule in biology (1–3). It is enzymatically synthesized from L-arginine (Arg) by NO synthases (NOSs). The NOSs typically show a bidomain structure in which an N-terminal oxygenase domain containing binding motifs for iron protophyrin IX (heme), (6*R*)-tetrahydrobiopterin (H4B), and Arg is fused to a C-terminal reductase domain that contains binding sites for FMN, FAD, and NADPH. A calmodulin (CaM) binding site is located between the oxygenase and reductase domains. The NOS oxygenase and reductase domains can be separately expressed in *Escherichia coli* and fold and function independent of one another. This has facilitated biochemical, biophysical, and crystallographic studies of each domain (4–11).

Conversion of Arg to NO occurs in two steps that involve an initial formation of N^{ω}-hydroxy-L-arginine (NOHA) as an enzyme-bound intermediate, followed by its further oxidation to NO and citrulline (12–14). Both steps require transfer of NADPH-derived electrons from the reductase domain flavins to the heme group in the oxygenase domain, which is bound to the protein through a cysteine thiolate axial ligation as in the cytochromes P450 (15–18). In the reductase domain, NADPH first reduces FAD, which shuttles electrons to FMN. The FMN to heme electron transfer in neuronal NOS (nNOS) and endothelial NOS (eNOS) is triggered by CaM binding (19–21) and is imperative for catalysis because it enables the heme iron to bind and activate oxygen in both steps of the reaction sequence. In nNOS and eNOS, CaM binding requires elevated Ca^{2+} and is readily reversible, whereas CaM binding to inducible NOS (iNOS) occurs at extremely low Ca^{2+} concentrations and is essentially irreversible (22, 23). Thus, nNOS or eNOS has typically been used to investigate the mechanism of CaM activation in NOS (19, 23–28).

NOS are only active in dimeric form. It is therefore critical to explore why and how dimerization influences their catalysis. Various aspects of dimerization have mainly been studied in nNOS and iNOS. In order to dimerize, nNOS and iNOS monomers must first incorporate heme, and the dimeric NOS structure is further stabilized by binding H4B and Arg (29–31). The dimeric interaction primarily involves the oxygenase domains of two subunits, with the reductase domains interacting loosely as monomeric tails (32). The electron transfer pathway between the reductase and oxygenase domains in a dimer has only been established for iNOS (33, 34). It proceeds from the FMN of one subunit to the heme bound in the partner subunit of the dimer. Thus, in iNOS heme reduction occurs exclusively "in *trans*," and this helps explain why dimerization is required for its activity. However, it is not known if heme reduction occurs through the same path in other NOS isoforms, and it is unclear how CaM binding might control the process.

To address these issues, we generated and characterized four nNOS heterodimers composed of a full-length subunit and a nNOSoxy partner subunit. Such heterodimers have a single reductase domain attached to a dimeric oxygenase domain. The heterodimers contained point mutations to inhibit homodimer formation (G671A) or prevent Arg binding (E592A) (Fig. 1). In addition, we utilized a soybean CaM protein and CaM-troponin C chimeras that are known to support different rates of heme reduction in wild type nNOS relative to mammalian CaM (25,

* This work was supported by National Institutes of Health Grants CA53914 and GM51491 (to D. J. S.). The costs of publication of this article were defrayed in part by the payment of page charges. This article must therefore be hereby marked "*advertisement*" in accordance with 18 U.S.C. Section 1734 solely to indicate this fact.

‡ To whom correspondence should be addressed: Immunology NB-3, Lerner Research Institute, Cleveland Clinic, 9500 Euclid Ave., Cleveland, OH 44195. Tel.: 216-445-6950; Fax: 216-444-9329; E-mail: stuehrd@ccf.org.

[1] The abbreviations used are: NO, nitric oxide; NOS, nitric-oxide synthase; nNOS, neuronal nitric-oxide synthase; eNOS, endothelial nitric-oxide synthase; iNOS, inducible nitric-oxide synthase; Arg, L-arginine; CaM, calmodulin; H4B, (6*R*)-5,6,7,8-tetrahydro-L-biopterin; EPPS, 4-(2-hydroxyethyl)-1-piperazinepropanesulfonic acid; FL, full-length NOS subunit; OXY, oxygenase subunit; WT, wild type; NOHA, N^{ω}-hydroxy-L-arginine; DTT, dithiothreitol; ScaM1 V144M, soybean calmodulin point mutant V144M.

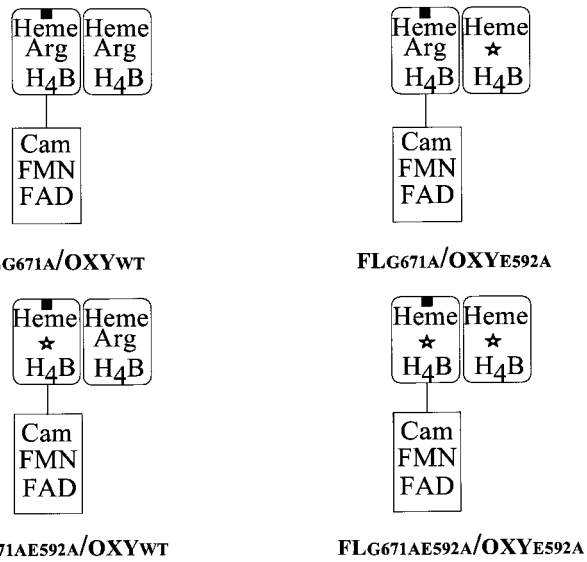

FIG. 1. **The four complementary heterodimers used in this study.** Each heterodimer is comprised of a full-length and oxygenase domain subunit. Two oxygenase domains (*rounded squares*) form the dimer interface and bind heme, H4B, and Arg, whereas the single reductase domain (*rectangle*) binds CaM, FMN, FAD, and NADPH. All full-length subunits contain the G671A mutation (*solid square*). Full-length or oxygenase domain subunits may also contain the Arg binding mutation E592A (*star*).

35) to probe how CaM binding controls electron transfer in the heterodimer. The results clearly establish the path of electron transfer between flavin and heme groups in nNOS and reveal how CaM binding regulates heme reduction by the single reductase domain.

EXPERIMENTAL PROCEDURES

Materials—All reagents and materials were obtained from Sigma or sources previously reported (33–35). Soybean CaM-1 point mutant V144M was a gift from Dr. J. David Johnson (Biochemistry Department, Ohio State University). L-NOHA was a gift from Dr. Bruce King (Chemistry Department, Wake Forest University). The CaM-cardiac troponin C (CaMTnC) chimeras CaM1TnC, CaM2TnC and CaM3TnC (number refers to the CaM domain that is replaced by an analogous TnC domain in the chimera) were expressed in *E. coli* and prepared as previously described (36).

Molecular Biology—Wild type and mutant nNOS containing a His_6 tag attached to their N terminus were overexpressed in *E. coli* strain BL21 (DE3) using a modified pCWori vector as described (25, 35). Restriction digestions, cloning, and bacterial growth were performed using standard procedures (38). Transformations were done using TransformAid kit from MBI Fermentas. Site directed mutagenesis was done using the QuickChange polymerase chain reaction *in vitro* mutagenesis kit from Stratagene. Incorporated mutations were confirmed by DNA sequencing at the Yale University DNA sequencing facility. DNAs containing the desired mutations were transformed into *E. coli* strain BL21 (DE3) for protein expression.

Oligonucleotides used to construct site-directed mutants in nNOS were synthesized by Integrated DNA Technologies. Silent mutations coding for restriction sites were incorporated in the mutated oligonucleotides to aid screening. Mutations (boldface type), silent restriction sites (underlined), and their corresponding oligonucleotides were as follows: G671A-*Bam*HI-sense, *p*-GAGGG**GCC**TGCCCCGCCGACTGGGTGTGGATTGTGCCTCCCATGTCGGGATCCATCACCCCTG; G671A-antisense, *p*-CAGGGGTGATGGATCCCGACATGGGAGGCACAATCCACA CCCAGTCGGCGGGGCAGGCCCCTC; E592A-*Kpn*I-sense, *p*-TCAGCGGCTGGTACATGGGTACC**GCG**ATCGGCGTCCG; E592A-antisense, *p*-CGGACGCCGATCGCGGTACCCATGTACCAGCCGCTGA.

Expression and Purification of Wild Type and Mutant nNOS—Wild type and mutant nNOS were purified in the absence of H4B and Arg as described previously (25, 39). The UV-visible spectra were recorded on a Hitachi U3110 Spectrophotometer in the absence and presence of 10 mM Arg and 20 μM H4B. The ferrous heme-CO-adduct absorbing at 444 nm was used to quantitate heme protein content using an extinction coefficient of 74 mM^{-1} cm^{-1} (A_{444}–A_{500}).

Gel Filtration—Dimer and monomer content of the mutant full-length nNOS proteins were estimated using an Amersham-Pharmacia Superdex 200HR column equilibrated with 40 mM EPPS, pH 7.6, containing 10% glycerol, 3 mM DTT, and 0.25 M NaCl after overnight incubation of the proteins with and without Arg (10 mM) and H4B (100 μM). Molecular weights of the protein peaks were estimated relative to protein molecular weight standards.

Preparation of nNOS Heterodimers—Wild type nNOSoxy or nNOSoxyE592A proteins were first incubated at a concentration of 30–40 μM with 3 M urea in 40 mM EPPS, 3 mM DTT, and 10% glycerol for 2.5 h at 15 °C to generate their monomers. The samples were then diluted 10-fold with 40 mM EPPS, 10% glycerol, and 3 mM DTT and incubated at different concentrations (0–1.5 μM) with 0.3 μM of full-length G671A nNOS or full-length G671A/E592A nNOS. To promote dimerization, 200 μM H4B and 20 mM Arg were added to the protein mixtures to give a final volume of 50 μl, and the samples were incubated for 1 h at 30 °C. Antagonist experiments were done with the G671A and G671A/E592A full-length mutants the same way, except they also included 0.3 μM wild type nNOSoxy monomer in each well. Large scale heterodimer preparations for measuring heme reduction were made by scaling up the total volume to 1 ml and upgrading the full-length protein concentration to 3 μM and the oxy domain monomer concentration to 6 μM.

Low Temperature SDS-Polyacrylamide Gel Electrophoresis—Formation of a heterodimer from G671A and nNOSoxy subunits was investigated using the low temperature method of Klatt *et al.* (30) with modifications. Protein samples were mixed with 20 μl of sample buffer containing 0.125 M Tris-HCl (pH 6.8), 4% (w/v) SDS, 20% (w/v) glycerol, and 0.02% (w/v) bromphenol blue and subjected to SDS-polyacrylamide gel electrophoresis in an ice-water bath at a constant current of 16 mA on 1-mm slab gels (7 × 8 cm) using a Mini Protean II apparatus from Bio-Rad. Gels and buffers were equilibrated at 4 °C prior to electrophoresis. In a separate experiment, the same samples were boiled in the additional presence of 10% (v/v) β-mercaptoethanol before being subjected to SDS-polyacrylamide gel electrophoresis under similar conditions as described above. Subsequently, gels were stained for protein with Coomassie Blue R-250. The apparent molecular mass of the heterodimer and its component G671A and nNOSoxy subunits were determined using the Bio-Rad prestained SDS-polyacrylamide gel electrophoresis standards myosin (subunit mass 197 kDa), β-galactosidase (subunit mass 115 kDa), bovine serum albumin (subunit mass 89 kDa), and ovalbumin (subunit mass 52 kDa).

NO Synthesis and NADPH Oxidation—After the incubation to promote dimerization, heterodimer NO synthesis was assayed in 96-microwell plates by diluting each sample to 100 μl with assay buffer such that each well contained a final concentration of 40 mM EPPS, 3 mM DTT, 4 μM FAD, 4 μM FMN, 200 μM H4B, 20 mM Arg, 0.9 mM EDTA, 1.2 mM Ca^{2+}, 0.9 μM CaM, 1 mg/ml bovine serum albumin, 18 units/ml catalase, and 10 units/ml superoxide dismutase. NADPH (1 mM) was added to each well to start the reaction. These were then incubated at 37 °C for 30 min, and the reaction was stopped by enzymatic oxidation of NADPH. Griess reagent (0.1 ml) was added to each well, and the absorbance was measured at 550 nm in a microplate reader. Nitrite produced by the heterodimers was quantified using $NaNO_2$ standards. In some cases, the heterodimer NO synthesis was also assayed using the spectrophotometric oxyhemoglobin assay (16, 34). After the dimerization incubation, sample aliquots were transferred into cuvettes containing 40 mM EPPS (pH 7.6), 0.3 mM DTT, 4 μM FAD, 4 μM FMN, 100 μM H4B, 10 mM Arg, 1 mg/ml bovine serum albumin, 0.8 mM Ca^{2+}, 0.6 mM EDTA, 0.9 μM CaM, 100 units/ml catalase, 10 units/ml superoxide dismutase, 5 μM oxyhemoglobin, and 300 μM NADPH in a total reaction volume of 300 μl. Heterodimer concentration was maintained at 0.2 μM in the cuvette. The reactions were initiated by adding NADPH and run for 3 min at 37 °C. The NO-mediated conversion of oxyhemoglobin to methemoglobin was monitored at 401 nm and converted to a rate of NO synthesis using a difference extinction coefficient of ϵ_{401} = 38 mM^{-1} cm^{-1}. Similar assays contained ScaM1 V144M protein or CaMTnC chimeras at 3 μM final concentration. NADPH oxidation rates were measured at 340 nm in the presence of oxyhemoglobin under identical conditions, and the rate of NADPH oxidation was calculated using an extinction coefficient of ϵ_{340} = 6.2 mM^{-1} cm^{-1}.

H_2O_2-dependent NOHA Oxidation—H_2O_2-dependent nNOS oxidation of NOHA to nitrite was assayed in 96-well microplates at 37 °C as described previously (39) with modification. The assay volume was 100 μl and contained 40 mM EPPS, pH 7.6, 300 nM nNOS heterodimer or homodimeric nNOS, 1 mM NOHA, 1 mM DTT, 25 units/ml superoxide dismutase, and 100 μM H4B. Reactions were initiated by adding 30 mM

H_2O_2 and stopped after 10 min incubation at 37 °C by adding 1300 units of catalase. Nitrite was detected at 550 nm after adding Griess reagent (100 μl) and quantitated based on nitrite standards.

Reduction of Heme Iron—All samples were equilibrated at 25 °C under anaerobic conditions in EPPS buffer (pH 7.6) saturated with CO. The cuvette contained a heterodimer formed from 3 μM of either G671A or G671A/E592A full-length mutant with 6 μM wild type nNOSoxy, in CO-saturated 40 mM EPPS buffer, pH 7.6, containing 0.5 mM DTT, 100 μM H4B, 10 mM Arg, 3 μM CaM, 0.9 mM Ca^{2+}, and 0.6 mM EDTA. Concentrated anaerobic NADPH solution was added to a final concentration of 0.1 mM, and successive spectral measurements were recorded. After spectral change had stopped, a small amount of dithionite solution was added, and the spectrum was recorded again. Heme reduction was measured as the absorbance difference between 444 and 500 nm and was quantitated using the initial spectrum recorded without NADPH as a base line and the dithionite-reduced spectrum as representing 100% reduced heme.

Arg Binding—Arg binding affinity was studied at room temperature by perturbation difference spectrometry according to methods described previously (6, 40). The buffer contained 40 mM EPPS, 10% glycerol, 1 mM DTT, 10 μM H4B, and 2 μM enzyme. 1 mM imidazole was added to the cuvette prior to titration with Arg (0–1 M). The K_d of Arg was calculated by double reciprocal analysis of the absorbance differences *versus* substrate concentration.

RESULTS

Characterization of nNOS Mutants G671A, G671A/E592A, and nNOSoxyE592A—The G671A mutation in rat nNOS is analogous to the previously characterized G450A mutation in mouse iNOS, which completely inhibits homodimer formation but permits heterodimer formation with either wild type monomers or monomers that contain a distinct mutation (34, 40–43). We thus hoped that G671A nNOS would display a similar phenotype to facilitate heterodimer formation. The nNOS E592A mutation is analogous to the previously characterized E371A mutation in mouse iNOS and E361A mutation in human eNOS. Both mutations completely prevent Arg binding in homodimeric NOS (6, 44), and studies with iNOS show that a heterodimer containing only one E371A mutation displays normal Arg binding in the partner subunit that does not contain this mutation (34). This is consistent with crystal structure data showing that Glu^{371} is a key protein residue that holds substrate Arg above the heme in the active site by forming hydrogen bonds between its carboxylate group and two guanidino nitrogens of Arg (9–11). Because this Glu residue is highly conserved among all NOS isoforms (6, 44), we expected that its mutation would also prevent Arg binding in nNOS.

Gel filtration of full-length nNOS mutants purified in the absence of Arg and H4B showed that G671A was predominantly monomeric but still contained some detectable dimer, whereas the E592A/G671A double mutant was almost completely monomeric (Fig. 2). In comparison, wild type nNOS purified under identical conditions was predominantly dimeric (Fig. 2, *inset*), consistent with previous reports (29, 30, 45). The gel filtration profiles of G671A and the double mutant did not change after incubating the proteins overnight with 10 mM Arg or 100 μM H4B alone or in combination (Fig. 2). Gel filtration of nNOSoxyE592A showed that it was predominantly dimeric (data not shown), consistent with the analogous iNOS mutant (6). We conclude that (*a*) the G671A mutation causes a partial defect in nNOS homodimer formation that cannot be overcome by Arg or H4B and (*b*) the E592A mutation does not prevent nNOS dimer formation.

UV-visible spectra of purified nNOS G671A, G671A/E592A, and nNOSoxyE592A under various conditions are shown in Fig. 3. Reduction by dithionite in the presence of CO allowed formation of ferrous heme-CO complex absorbing at 444 nM for all three proteins (Fig. 3, *insets*). This indicates proper heme incorporation with cysteine thiolate axial ligation. Spectra of the ferric proteins in buffer containing DTT show a split Soret

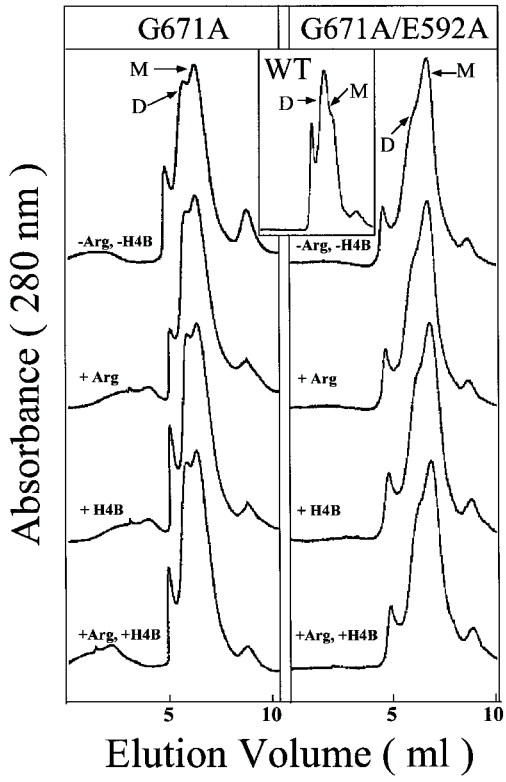

FIG. 2. **Gel filtration profiles of G671A and G671A/E592A full-length nNOS.** 50 μg of the purified mutants were loaded on a Superdex 200 HR column as described under "Experimental Procedures." Proteins were preincubated with H4B and/or Arg as indicated. The three peaks in each trace eluting between 4 and 8 ml represent (from *left* to *right*) protein aggregate, homodimer (*D*), and monomer (*M*). Results shown are representative of three similar experiments.

absorbance at 380 and 460 nM in all cases. This is characteristic of a bis-thiolate in which the ferric NOS heme iron has bound DTT (46). There is also some absorbance present at 415–430 nm in the spectra of G671A and nNOSoxyE592A that is due either to incomplete DTT binding or some binding of imidazole carried over from the purification. Adding Arg alone brought about a weak but discernible shift in the spectrum of G671A that indicated displacement of bound DTT by Arg and a shift toward a high spin state (Fig. 3, *trace B*, *upper panel*). Adding Arg failed to produce this change in the spectra of G671A/E592A or nNOSoxyE592A mutants (*trace B*, *middle* and *lower panels*). The addition of H4B alone caused a shift in the spectra toward high spin in all three mutants, indicating that H4B displaced some bound DTT (*trace C*, *all panels*). The H4B effect was most prominent in nNOSoxyE592A, consistent with this protein being predominantly dimeric. Further addition of Arg to the H4B-bound proteins slightly increased the high spin character of G671A (*trace D*, *upper panel*) but did not cause any change in the spectra of G671A/E592A or nNOSoxyE592A (*trace D*, *middle* and *lower panels*). Arg was also unable to displace imidazole bound to the heme in nNOSoxyE592A (data not shown). These results, in light of the gel filtration data, suggest that the G671A mutation limits Arg and H4B binding by inhibiting nNOS dimerization, whereas the E592A mutation specifically inhibits Arg binding without an effect on dimerization. The nNOS mutants therefore display the expected phenotypes, with the exception that the G671A mutation did not completely prevent nNOS homodimer formation.

The G671A mutant had a very low but detectable NO synthesis activity as measured by the oxyhemoglobin spectroscopic assay (3% of wild type nNOS, Table I). This is consistent with our spectral data indicating that its small dimeric fraction is able to

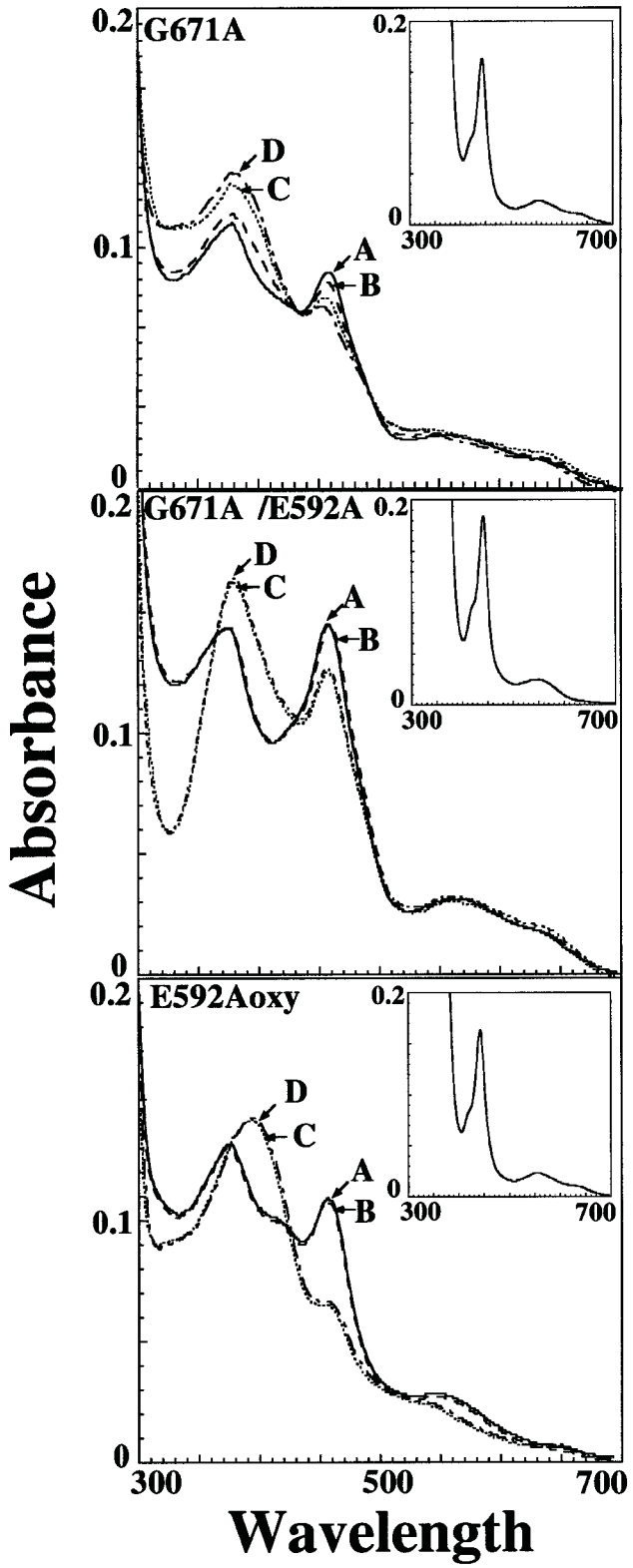

FIG. 3. **Light absorption spectra of G671A, G671A/E592A, and nNOSoxyE592A in the presence and absence of Arg and H4B.** Protein spectra were recorded at 25 °C after dilution in buffer containing 2 mM DTT alone (*A*) or after incubating the proteins overnight at 4 °C in buffer containing DTT plus 10 mM Arg (*B*), 20 μM H4B (*C*), or both Arg and H4B (*D*). *Insets* show the spectrum of the dithionite-reduced, ferrous heme-CO complex of each mutant.

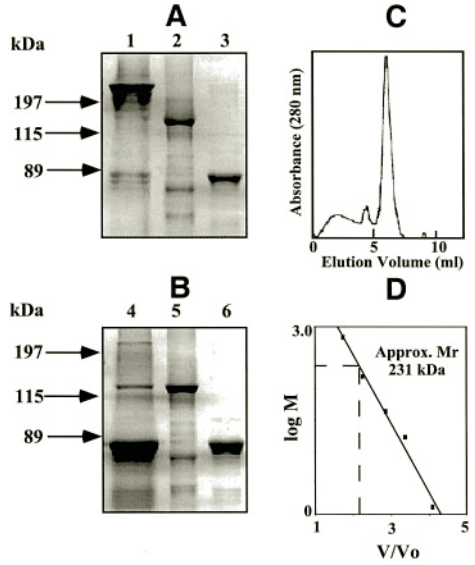

FIG. 4. **Low temperature gel electrophoresis and gel filtration of FLG671AOXY$_{WT}$ heterodimer.** Approximately 20 μg of heterodimer (*lane 1*), 10 μg of G671A (*lane 2*), and 10 μg of urea-generated nNOSoxy monomer (*lane 3*) samples were analyzed by gel electrophoresis without boiling (*A*) or after being boiled in the presence of β-mercaptoethanol (*B*, *lanes 4-6*). Proteins were stained with Coomassie Blue. The *arrows* indicate positions of molecular weight standards. See "Experimental Procedures" for details. *C*, elution profile of the heterodimer during gel filtration chromatography. *D*, calculation of heterodimer apparent molecular mass relative to gel filtration standards thyroglobulin (670 kDa), bovine γ-globulin (158 kDa), chicken ovalbumin (44 kDa), equine myoglobin (17 kDa), and vitamin B-12 (1.35 kDa).

bind H4B and Arg. There was no detectable increase in its activity after incubating overnight with 10 mM Arg and 20 μM H4B, in keeping with this incubation not increasing dimer content (see Fig. 2). The nNOS double mutant G671A/E592A has no detectable NO synthesis activity (Table I), consistent with its being primarily monomeric and completely unable to bind Arg. H_2O_2-dependent L-NOHA oxidation to nitrite activities essentially mirrored the NO synthesis results (0.68 ± 0.42 min^{-1} for G671A and undetectable for both G671A/E592A and nNOSoxyE592A, compared with 22.7 ± 1.8 min^{-1} for wild type nNOS).

Both G671A and the double mutant displayed weak NADPH oxidation upon CaM binding in the presence of H4B and Arg and virtually no NADPH oxidation in the absence of CaM (Table I). NADPH supported only trace heme iron reduction in G671A or G671A/E592A mutants as determined by CO binding under anaerobic conditions (data not shown). These data indicate that heme reduction in nNOS requires dimerization, as is also true for iNOS (33, 34).

Generation of nNOS Heterodimers—To determine the path of electron transfer in nNOS, we generated four different heterodimers by combining full-length subunits of G671A or G671A/E592A with subunits of either wild type nNOSoxy or E592A nNOSoxy (Fig. 1). The dimeric nNOSoxy proteins were first dissociated into heme-containing monomers using 3 M urea, diluted, and then mixed with the complementary full-length subunits. Full-length G671A and G671A/E592A mutants were used without urea pretreatment in our heterodimer experiments.[2] H4B and Arg were then added to promote dimerization of subunits. As shown in Fig. 4*A*, this generated a SDS-resistant heterodimer whose estimated molecular mass (~235 kDa) matched the molecular mass as calculated from the amino acid sequence (241 kDa). The heterodimer dissociated when boiled under reducing conditions (Fig. 4*B*) and eluted as a single peak during gel filtration under native conditions (Fig.

[2] Although treating G671A nNOS with 3 M urea completely dissociated its residual dimer fraction (data not shown), we found that this treatment did not increase heterodimer formation relative to using G671A protein as purified.

TABLE I

NO synthesis and NADPH oxidation by G671A, G671A/E592A, and their heterodimers in the presence and absence of CaM

NO synthesis and NADPH oxidation were measured at 25 °C. Measurements and analysis are detailed under "Experimental Procedures." All values are turnover numbers per full length subunit heme, and are the mean ± S.D. for three independent measurements.

System	NO synthesis		NADPH oxidation	
	With CaM	Without CaM	With CaM	Without CaM
	min^{-1}		*min*$^{-1}$	
$nNOS_{WT}$	23.6 ± 0.7	Nil	55.8 ± 0.8	3.0 ± 0.9
G671A only	0.76 ± 0.01	Nil	7.3 ± 0.02	0.84 ± 0.1
G671A/E592A only	Nil	Nil	6.0 ± 0.01	0.75 ± 0.03
FL_{G671A}/OXY_{WT}	10.5 ± 0.3	Nil	53.8 ± 0.9	7.2 ± 0.1
$FL_{G671A/E592A}/OXY_{WT}$	9.7 ± 0.4	Nil	51.5 ± 2.2	6.9 ± 0.3
FL_{G671A}/OXY_{E592A}	Nil	Nil	47.7 ± 0.3	6.7 ± 0.03
$FL_{G671A/E592A}/OXY_{E592A}$	Nil	Nil	44.6 ± 0.9	6.6 ± 0.4

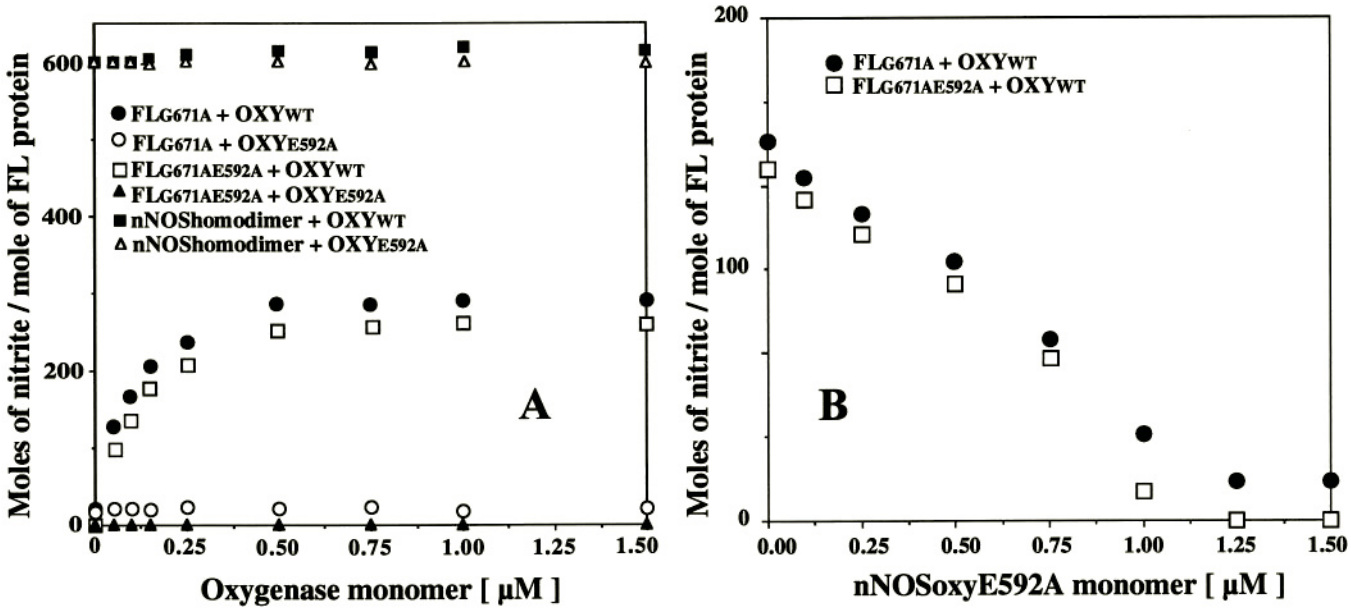

FIG. 5. **Heterodimer complementation and antagonism assays.** *A*, complementation. G671A, G671A/E592A, or wild type nNOS homodimer (0.3 μM) was preincubated with the indicated concentrations of nNOSoxy monomer or nNOSoxyE592A monomer in the presence of Arg and H4B. Catalytic activity (nitrite formation) was then assayed in a 30-min reaction. *B*, antagonism. G671A or G671A/E592A (0.3 μM) was preincubated with the indicated concentrations of nNOSoxyE592A monomer in the presence of 0.3 μM nNOSoxy monomer. Catalytic activity (nitrite formation) was then assayed in a 30-min reaction. See "Experimental Procedures" for details. Values are mean of three independent experiments, the S.D. averaged <10%.

4*C*) with estimated molecular mass of 231 kDa (Fig. 4*D*).

Incorporating the E592A Arg binding mutation into both, none, or either of the oxygenase domains in the heterodimer allows NO synthesis to become a marker to identify which heme(s) receive electrons from the single reductase domain. Specifically, if both hemes can be reduced, then three of the heterodimers should be active and one ($FL_{G671A/E592A}/OXY_{E592A}$) should not (see Fig. 1). If only the heme that is adjacent to the reductase domain is reduced (as occurs in iNOS; Refs. 33 and 34), then two of the heterodimers should be active (FL_{G671A}/OXY_{WT} and $FL_{G671A/E592A}/OXY_{WT}$), and two should not ($FL_{G671A}/OXY_{E592A}$ and the $FL_{G671A/E592A}/OXY_{E592A}$). If only the heme present in the same subunit as the reductase domain is reduced, then a different heterodimer pair should be active (FL_{G671A}/OXY_{WT} and FL_{G671A}/OXY_{E592A}).

NO Synthesis and NADPH Oxidation—Fig. 5*A* shows specific activities (nitrite synthesis from Arg) in four complementation reactions where either the G671A or G671A/E592A full-length mutants were induced to dimerize with increasing concentrations of either wild type nNOSoxy or E592A nNOSoxy subunits (see Fig. 1 for heterodimer composition). It is apparent from the curves that the FL_{G671A}/OXY_{WT} and $FL_{G671A/E592A}/OXY_{WT}$ complementation reactions became active, while the FL_{G671A}/OXY_{E592A} and $FL_{G671A/E592A}/OXY_{E592A}$ reactions were no more active than the parent full-length subunits. Identical results were obtained when CaM was or was not bound to the full-length subunits during the dimerization incubation (data not shown). Maximum activities attained by the FL_{G671A}/OXY_{WT} and $FL_{G671A/E592A}/OXY_{WT}$ heterodimers were about half the value we obtained with a wild type nNOS homodimer in the same assay (600 mol of nitrite/mol of heme; Fig. 5*A*).

To examine if the low activity in the latter two heterodimer reactions was due to a dimerization defect, we carried out an antagonism study (40, 43) whereby we examined the ability of nNOSoxyE592A monomers to compete with a fixed amount of wild type nNOSoxy in forming a heterodimer with G671A as well as the G671A/E592A full-length subunits (Fig. 5*B*). This showed that nNOSoxyE592A monomers lowered the specific activity achieved in the complementation reaction in a concentration-dependent manner, down to levels that were close to the maximum activities obtained in Fig. 5*A* for each of the full-length mutants alone. Their good ability to compete with wild type nNOSoxy monomers indicates that E592A monomers were able to form heterodimers with the full-length subunits. Together, these results argue against the single reductase domain transferring electrons to both hemes or to the heme in the same subunit. Rather, they support electron transfer only to the heme in the adjacent subunit and suggest that this enables oxidation of Arg at a normal rate within the adjacent subunit.

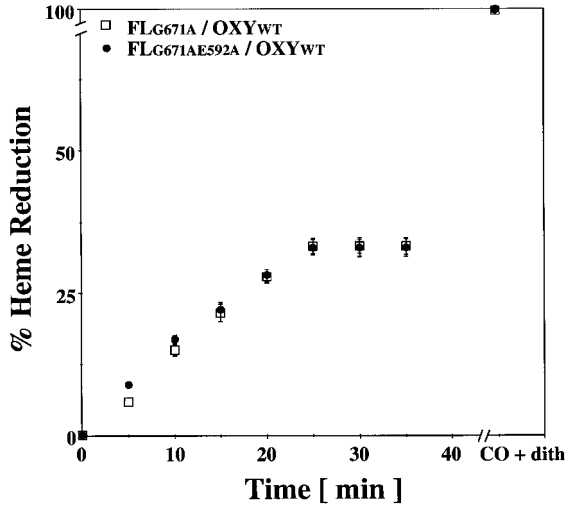

FIG. 6. **Heme reduction in FL_{G671A}/OXY_{WT} and $FL_{G671A/E592A}/OXY_{WT}$ heterodimers.** Heterodimers were made by incubating 3 μM full-length proteins with 6 μM nNOSoxy monomer in the presence of Arg, H4B, excess Ca^{2+}, and CaM. Samples were made anaerobic and were saturated with CO. Heme reduction was initiated by adding NADPH, and spectra were recorded at the indicated times. After 35 min, dithionite solution was added, and a spectrum was recorded to determine total reducible heme in the cuvette (expressed as 100% in the *figure*). See "Experimental Procedures" for details. The results shown are representative of three independent experiments.

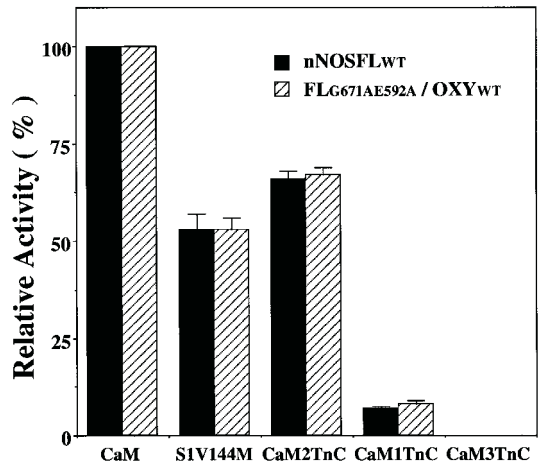

FIG. 7. **NO synthesis by nNOS homodimer and heterodimer in response to CaM and four CaM substitute proteins.** Rates of NO synthesis were measured using the oxyhemoglobin assay. Rates are expressed on a per active heme basis and are relative to each protein's response to wild type CaM (100% value). See "Experimental Procedures" for details. Data are the mean ± S.D. of four independent experiments.

Table I compares NO synthesis activities of the four heterodimers as assayed by the oxyhemoglobin method, along with their NADPH oxidation rates in the presence and absence of CaM. The NO synthesis assays match results obtained in the nitrite assays of Fig. 5*A*; namely, the FL_{G671A}/OXY_{WT} and $FL_{G671A/E592A}/OXY_{WT}$ heterodimers were equally active, while the other two heterodimers were not active. Also, here the heterodimers were again almost half as active on a per heme basis as wild type nNOS. Interestingly, NADPH consumption was increased in a CaM-dependent manner in all four heterodimers irrespective of their NO synthesis. This suggests that CaM triggers heme reduction in the heterodimers even in the absence of substrate, as is true for wild type nNOS (20). That NADPH consumption in the presence of CaM was predominantly implicated with heme reduction was confirmed by the fact that an Arg analogue that blocks heme reduction in nNOS (N^{ω}-nitro-L-arginine methyl ester; Refs. 47 and 48) inhibited NADPH oxidation of the FL_{G671A}/OXY_{WT} heterodimer by about 78% (data not shown).

NADPH-dependent Heme Iron Reduction—We next examined the FL_{G671A}/OXY_{WT} and $FL_{G671A/E592A}/OXY_{WT}$ heterodimers regarding their NADPH-dependent heme iron reduction in the presence of CO under anaerobic conditions. Heterodimers were formed by combining 3 μM full-length subunits with 6 μM oxygenase domain monomer in the presence of Arg and H4B. Fig. 6 plots the time-dependent formation of a ferrous heme-CO complex after adding NADPH to either heterodimer. In both cases, reduced heme reached a maximum that represented about 30–35% of the total heme present in the cuvette (determined by adding dithionite at the end of the experiment). This result is consistent with the relative proportion of full-length and oxygenase subunits in the reactions and suggests that all of the full-length subunits formed a heterodimer that catalyzed transfer of NADPH electrons to the heme located only in the adjacent subunit.

Ability of CaM Substitutes to Support Heterodimer NO Synthesis—We investigated the role of CaM in controlling heterodimer heme reduction by comparing the abilities of four substitute CaMs to support NO synthesis. These four substitutes (ScaM-1 V144M and CaMTnC chimeras CaM2TnC, CaM1TnC, and CaM3TnC) all bind tightly to wild type nNOS (36) and are known to support a range of slower NO synthesis and heme reduction rates (25, 35), with the exception of CaM3TnC, which supports no heme reduction or NO synthesis. As shown in Fig. 7, the $FL_{G671A/E592A}/OXY_{WT}$ heterodimer responded the same as wild type nNOS toward the four CaM substitutes regarding rate of NO synthesis.

DISCUSSION

Electron transfer in our nNOS heterodimer occurred only between the reductase and oxygenase domains of opposite subunits and resulted in a normal rate of catalysis by the reduced heme. This conclusion is uniquely consistent with (*a*) the NO synthesis pattern we observed among the four heterodimers, (*b*) their maximum rate of NO synthesis (~50% of a nNOS homodimer), and (*c*) their extent of NADPH-dependent heme reduction (only one of two hemes was reduced). Our finding helps explain why nNOS must dimerize to support heme reduction and catalyze NO synthesis. Because iNOS has an identical structural constraint regarding its heme reduction (34, 35), our results imply that intersubunit electron transfer is a general feature among the NOSs.

The heterodimer also helps to clarify some aspects of reductase domain and CaM function in nNOS. For example, the simple absence of a second attached reductase domain did not allow heme reduction to occur; nor did it alter catalysis by the heme once it received electrons upon CaM binding. Thus, reductase domains do not influence either reduction or function of the oxygenase domains to which they are covalently attached. Rather, the single reductase domain in the full-length subunit could only interact productively with the oxygenase domain in the adjacent subunit. This process was differentially controlled by CaM and four CaM substitute proteins that are known to bind well to nNOS homodimer and support a range of slower heme reduction rates. Remarkably, the four CaM proteins affected the heterodimer in exactly the same manner as the nNOS homodimer. They supported NO synthesis in the same rank order (CaM > CaM2TnC > ScaM1 V144M > CaM1TnC ≫ CaM3TnC) and each supported an identical rate of NO synthesis (per active heme) in four of four circumstances. Such close identity between nNOS heterodimer and homodimer strongly implies that CaM binding activates heme reduction

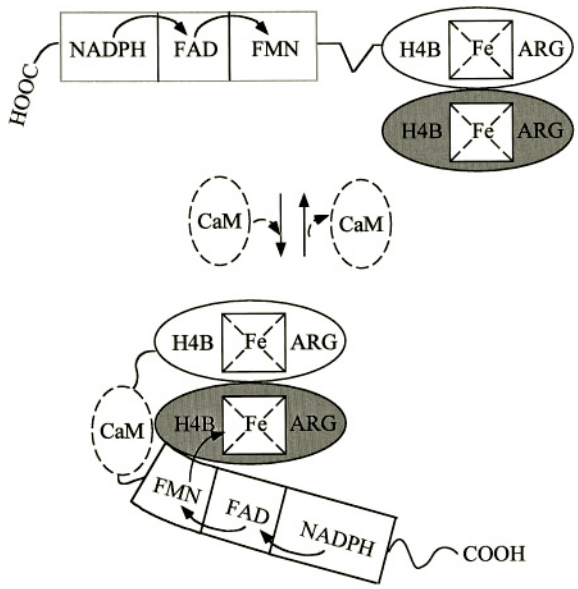

FIG. 8. **CaM-induced electron transfer in a nNOS heterodimer.** In the absence of CaM, the nNOS protein prevents electron transfer between the single reductase domain and either heme in the heterodimer. CaM binding enables electron transfer between FMN and the heme located on the adjacent subunit.

through an identical mechanism in both proteins. A model for CaM function consistent with our results is shown in Fig. 8.

CaM binding does not alter the thermodynamics of electron transfer in nNOS (49) but instead removes a kinetic barrier to heme reduction. The heterodimer reveals that CaM does so by allowing a productive interaction to occur between reductase and oxygenase domains on adjacent subunits. However, it is interesting to note that CaM binding still does not remove the kinetic barrier toward heme reduction within the same subunit. Recently, autoinhibitory control elements have been identified in the FMN module and the extreme C terminus of the nNOS reductase domain (28, 50–52). These elements must help establish a kinetic barrier to heme reduction, because removal of either element allows for some NO synthesis to occur in the absence of bound CaM (50–52). Although this suggests that the elements actively suppress electron transfer between reductase and oxygenase domains, it is unclear whether they do so within the same subunit, between adjacent subunits, or both. Heterodimer experiments similar to those reported here can resolve these possibilities.

The nNOS and iNOS heterodimers point out some interesting similarities and differences between NOS isoforms. For example, the E592A mutation completely prevented Arg binding and NO synthesis in the nNOS oxygenase domain that contained the mutation. Because this mutant phenotype matches the corresponding E371A mutation in mouse iNOS (6) and E361A mutation in human eNOS (44), it confirms that Glu^{592} performs an identical function in nNOS, namely to bind the guanidino group of Arg and hold it above the heme. Conservation of function matches the high sequence homology among NOS substrate binding helices, which all contain this Glu residue (6, 44).

G671A nNOS was partly dimeric (about 20%). This contrasts with the analogous iNOS G450A mutant that is 100% monomer (41, 42). The difference matches the fact that a nNOS dimer requires higher urea concentrations to dissociate than an iNOS dimer.[3] Indeed, available sequence and crystal structure data predict some differences among residues that make up the dimer interface in iNOS and nNOS, particularly around nNOS Gly^{671} and in the N-terminal hook (43, 53). These will be discussed in detail elsewhere.[4] Although G671A nNOS was not a complete monomer, its ability to form heterodimers with nNOS oxygenase subunits appeared complete (*i.e.* on a stoichiometric basis). Complete heterodimer formation would require residual G671A nNOS dimer to dissociate and may be favored for two reasons: (*a*) heterodimers contain only one dimer-destabilizing G671A mutation instead of two, and (*b*) heterodimers contain only one attached reductase domain instead of two (attached reductase domains destabilize the NOS dimer; Ref. 32).

In iNOS, dimer formation enables heme reduction in two ways; it permits intersubunit electron transfer as discussed above and also removes a thermodynamic block by creating productive H4B and Arg binding sites in the dimer (34, 48). The heme in an iNOS dimer is held at such a low potential that in the absence of H4B and (more importantly) Arg, its reduction by the flavins is not thermodynamically favored (48). In contrast, the heme in a nNOS dimer is held at a more positive potential and is reduced by the flavins even in the absence of Arg and H4B (48, 49). This is consistent with our observing fast NADPH oxidation by the nNOS heterodimer that contained an Arg binding mutation in both oxygenase domains. Thus, the primary barrier to heme reduction in nNOS is a kinetic one, and it is removed when the dimer binds CaM. However, since iNOS always contains bound CaM, its unique thermodynamic barrier lets Arg binding replace CaM as the major factor controlling its heme reduction.

From an evolutionary standpoint, it is interesting to imagine how NOS heme reduction came to depend on intersubunit electron transfer. In our previous report (34), we speculated that NOS may have become a bidomain monomer (fusion of reductase and oxygenase genes, as in cytochrome P450BM3) before becoming a homodimer. This circumstance would have intradomain electron transfer occurring in the monomer precursor and its being replaced by interdomain electron transfer after the enzyme became dimeric. However, genes encoding NOS oxygenase-like proteins have recently been discovered in three microorganisms, and at least one of the gene products is dimeric when expressed in *E. coli*.[5] This implies that NOS first achieved a dimeric structure and must have received electrons from an unattached redox partner, as is seen in most cytochrome P450s. In this circumstance, a later gene fusion event that linked NOS oxygenase and reductase domains would have immediately created a situation where interdomain electron transfer could take place.

Although the NOS reductase domain is quite similar to NADPH cytochrome P450 reductase, its electron transfer interactions are controlled differently. This is manifest by its Ca^{2+}/CaM requirement, its autoinhibitory structural elements, its relying exclusively on interdomain interaction, and its different utilization of negatively charged residues in "cluster 1" of its FMN module (54). The origin and basis of these differences is interesting from both evolutionary and protein structure-function standpoints. Heterodimer methods as outlined here can help to address these issues.

Acknowledgment—We thank Abigail Meade for expert technical assistance.

REFERENCES

1. MacMiking, J., Xie, Q. W., and Nathan, C. (1997) *Annu. Rev. Immunol.* **15,** 323–350
2. Harrison, D. G. (1997) *J. Clin. Invest.* **100,** 2153–2157

[3] K. Panda, S. Ghosh, and D. J. Stuehr, unpublished results.

[4] K. Panda and D. J. Stuehr, manuscript in preparation.

[5] S. Adak, K. Panda, and D. J. Stuehr, unpublished data.

3. Gross, S. S., and Wolin, M. S. (1995) *Annu. Rev. Physiol* **57,** 737–769
4. Abu-Soud, H. M., Wu, C., Ghosh D. K., and Stuehr, D. J. (1998) *Biochemistry.* **37,** 3777–3786
5. Salerno, J. C., Martasek, P., Roman, L. J., and Masters, B. S. S. (1996) *Biochemistry* **35,** 7626–7630
6. Gacchui, R., Ghosh, D. K., Wu, C., Parkinson, J. P., Crane, B. R., and Stuehr, D. J. (1997) *Biochemistry* **36,** 5097–5103
7. Ghosh, D. K., and Stuehr D. J. (1995) *Biochemistry* **34,** 801–807
8. Chen, P. F., Tsai, A. L., Berka, V., Wu, K. K. (1996) *J. Biol. Chem.* **271,** 14631–14635
9. Crane, B. R,, Arvai, A. S,, Ghosh D. K., Wu, C., Getzoff, E. D., Stuehr, D. J., and Tainer, J. A. (1998) *Science* **279,** 2121–2126
10. Raman, C. S., Li, H., Martasek P., Kral, V., Masters, B. S. S., and Poulos, T. M. (1998) *Cell* **95,** 939–995
11. Fischmann, T. O., Hruza, A., Niu, X. D., Fosetta, J. D., Lunn, C. A., Dolphin, E., Prongay, A. J., Reichter, P., Lundell, D. J., Narula, S. K., and Weber, P. C. (1999) *Nat. Struct. Biol.* **6,** 233–242
12. Griffith, O. W., and Stuehr, D. J. (1995) *Annu. Rev. Physiol.* **57,** 707–736
13. Marletta, M. A. (1993) *J. Biol. Chem.* **268,** 12231–12234
14. Mayer, B., and Hemmens, B. (1997) *Trends Biochem. Sci.* **22,** 477–481
15. White, K. A., and Marletta, M. A. (1992) *Biochemistry* **31,** 7160–7165
16. Stuehr, D. J., and Ikeda-Saito, M. (1992) *J. Biol. Chem.* **267,** 20547–20550
17. Sono, M., Stuehr, D. J., Ikeda-Saito, M., and Dawson, J. H. (1995) *J. Biol. Chem.* **270,** 19943–19948
18. McMillan, K., Bredt, D. S., Hirsch, D. J., Snyder, S. H., Clark, J. E., and Masters, B. S. S. (1992) *Proc. Natl. Acad. Sci. U. S. A.* **89,** 11141–11145
19. Abu-Soud, H. M., Yoho, L. L., and Stuehr, D. J. (1994) *J. Biol. Chem.* **269,** 32047–32050
20. Abu-Soud, H. M., and Stuehr, D. J. (1993) *Proc. Natl. Acad. Sci. U. S. A.* **90,** 10769–10772
21. Presta, A., Liu, J., Sessa, W. C., and Stuehr, D. J. (1997) *Nitric Oxide* **1,** 74–87
22. Cho, H. J., Xie, Q. W., Calaycay, J., Mumford, R. A., Swiderek, K. M., Lee, T. D., and Nathan, C. (1992) *J. Exp. Med.* **176,** 599–604
23. Venema, R. C., Sayegh, H. S., Kent, J. D., and Harrison, D. G. (1996) *J. Biol. Chem.* **271,** 6435–6440
24. Lee, S. J., and Stull, J. T. (1998) *J. Biol. Chem.* **273,** 27430–27437
25. Gacchui, R., Abu-Soud, H., Ghosh, D. K., Presta, A., Blazing, M. A., Mayer, B., George, S. E., and Stuehr, D. J. (1998) *J. Biol. Chem.* **273,** 5451–5454
26. García-Cardeña, G., Martasek, P., Masters, B. S. S., Skidd, P. M., Couet, J., Li, S., Lisanti, M. P., and Sessa, W. C. (1997) *J. Biol. Chem.* **272,** 25437–25440
27. Michel, J. B., Feron, O., Sacks, D., and Michel, T. (1997) *J. Biol. Chem.* **272,** 15583–15586
28. Salerno, J. C., Harris, D. E., Irrizarry, K., Patel, B., Morales, A. J., Smith, S. M., Martasek, P., Roman, L. J., Masters, B. S. S., Jones, C. L., Weissman, B. A., Lane, P., Liu, Q., and Gross, S. S. (1997) *J. Biol. Chem.* **272,** 29769–29777
29. Klatt, P., Pfeffer, S., List, B. M., Lehner, D. Glatter, O., Bachinger, H. P., Werner, E. R., Schmidt, K., and Mayer, B. (1996) *J. Biol. Chem.* **271,** 7336–7342
30. Klatt, P., Schmidt, K., Lehner, D., Glatter, O., Bachinger, H. P., and Mayer, B. (1995) *EMBO J.* **14,** 3687–3695
31. Baek, K. J., Thiel, B. A., Lucas, S., and Stuehr, D. J. (1993) *J. Biol. Chem.* **268,** 21120–21129
32. Ghosh, D. K., Abu-Soud, H. M., and Stuehr, D. J. (1996) *Biochemistry* **35,** 1444–1449
33. Siddhanta, U., Wu, C., Abu-Soud, H. M., Zhang, J., Ghosh, D. K., and Stuehr, D. J. (1996) *J. Biol. Chem.* **271,** 7309–7312
34. Siddhanta, U., Presta, A., Fan, B., Wolan, D., Rosseau, D. L., and Stuehr, D. J. (1998) *J. Biol. Chem.* **273,** 18950–18958
35. Adak, S., Santolini, J., Tikunova, S., Wang, Q., Johnson, J. D., and Stuehr, D. J. (2001) *J. Biol. Chem.* **276,** 1244–1252
36. Su, Z., Blazing, M. A., Fan, D., and George, S. E. (1995) *J. Biol. Chem.* **270,** 29117–29122
37. Wu, C, Zhang, J., Abu-Soud, H. M., Ghosh, D. K., and Stuehr, D. J. (1996) *Biochem. Biophys. Res. Commun.* **22,** 439–444
38. Sambrook, J., Fritsh, E. F., and Maniatis, T. (1989) *Molecular Cloning: A Laboratory Manual*, Cold Spring Harbor Laboratory, Cold Spring Harbor, NY
39. Adak, S., Wang, Q., and Stuehr, D. J. (2000) *J. Biol. Chem.* **275,** 33554–33561
40. Ghosh, S., Wolan, D., Adak, S., Crane, B. R., Kwon, N. S., Tainer, J. A., Getzoff, E. D., and Stuehr, D. J. (1999) *J. Biol. Chem.* **274,** 24100–24112
41. Cho, H. J., Martin, E., Xie, Q. W., Sassa, S., and Nathan, C. (1995) *Proc. Natl. Acad. Sci. U. S. A.* **92,** 11514–11518
42. Xie, Q. W., Leung, M., Fantes, M., Sassa, S., and Nathan C. (1996) *Proc. Natl. Acad. Sci. U. S. A.* **93,** 4891–4896
43. Ghosh, D. K., Crane, B. R., Ghosh, S., Wolan, D., Gacchui, R., Crooks, C., Presta, A., Tainer, J. A., Getzoff, E. D., and Stuehr, D. J. (1999) *EMBO J.* **18,** 6260–6270
44. Chen, P. F., Tsai, A. L., Berka, V., and Wu, K. K. (1997) *J. Biol. Chem.* **272,** 6114–6118
45. Gerber, N. C., and Ortiz de Montellano, P. R. (1995) *J. Biol. Chem.* **270,** 17791–17796
46. Ghosh, D. K., Wu, C., Pitters, E., Moloney, E. R., Mayer, B., and Stuehr, D. J. (1997) *Biochemistry* **36,** 10609–10619
47. Abu-Soud, H. M., Feldman, P. L., Clark, P., and Stuehr, D. J. (1994) *J. Biol. Chem.* **269,** 32318–32326
48. Presta, A., Weber-Main, A, M., Stankovich, M. T., and Stuehr, D, J. (1998) *J. Am. Chem. Soc.* **120,** 9460–9465
49. Nobel, M. A., Munro, A. W., Rivers, S. L., Robledo, L., Daff, S. N., Yellowlees, L. J., Shimizu, T., Sagami, I., Guillemette, G., and Chapman, S. K. (1999) *Biochemistry* **38,** 16413–16418
50. Montgomery, H. J., Romanov, V., and Guillemette, J. G. (2000) *J. Biol. Chem.* **275,** 5052–5058
51. Roman, L. J., Martasek, P., Miller, R. T., Harris, D. E., de la Garza, M. A., Shea, T. M., Kim, J. J. P. and Masters, B. S. S. (2000) *J. Biol. Chem.* **275,** 29223–29232
52. Daff, S., Sagami, I., Shimizu, T. (1999) *J. Biol. Chem.* **274,** 30589–30595
53. Crane, B. R., Rosenfeld, R. A., Arvai, A. S., Ghosh, D. K., Ghosh, S., Tainer, J. A., Stuehr, D. J., and Getzoff, E. D. (1999) *EMBO J.* **18,** 6271–6281
54. Adak, S., Ghosh, S., Abu-Soud, H. M., and Stuehr, D. J. (1999) *J. Biol. Chem.* **274,** 22313–22320